NANO LETTERS

2004
Vol. 4, No. 9
1605−1611

On the Line Widths of Vibrational Features in Inelastic Electron Tunneling Spectroscopy

Michael Galperin and Mark A. Ratner

Department of Chemistry, Northwestern University, Evanston, Illinois 60208

Abraham Nitzan*

School of Chemistry, The Sackler Faculty of Science, Tel Aviv University, Tel Aviv, 69978, Israel

Received May 6, 2004; Revised Manuscript Received July 5, 2004

ABSTRACT

We address the line shape and line widths observed in recent inelastic electron tunneling spectroscopy (IETS) experiments. The nonequilibrium Green function (NEGF) formalism is used to analyze the effect of the electron–phonon interaction on the tunneling spectra. We find that IETS line shapes are sensitive to junction parameters, in particular the position of the bridge electronic resonance and the molecule–lead coupling that may be controlled experimentally. Intrinsic IETS line widths are found to be dominated by the coupling of molecular vibrations to electron–hole pairs excitations in the lead(s) to which the molecule is bonded chemically. While estimated widths are of similar order of magnitude as observed in the recent experiment of Wang et al. (*Nano Lett.* 2004, *4*, 643), one cannot rule out inhomogeneous contribution to the line width in this monolayer experiment.

Inelastic electron tunneling spectroscopy (IETS) has been an important tool for identifying molecular species in tunnel junctions for a long time.[1,2] With the development and advances in scanning tunneling microscopy (STM) and spectroscopy (STS) it has proven invaluable as a tool for identifying and characterizing molecular species within the conduction region.[3−16] Indeed, this is the only direct way to ascertain that a molecular species participates in the conduction process and at the same time to provide important spectroscopic and structural data on the conducting molecule, in particular, information on the strength of the vibronic coupling itself.

Most past theoretical discussions of IETS are based on low order perturbative treatments[1,17−19,20] where the tunneling current is computed in the lowest order in the electron−phonon coupling. Such an approach is very useful for rough estimates using realistic molecular models, and, when carried out carefully, can qualitatively explain some subtle issues, e.g., the sometimes negative response in $d^2I/d\Phi^2$ (where I is the current and Φ is the imposed potential bias),[17−19] but it is not fully consistent with the nonequilibrium conditions under which such measurements are done as well as with the boundary restrictions imposed by the Pauli principle. Our present discussion is based on the nonequilibrium Green's function (NEGF) formulation,[21−24] which provides a systematic framework for describing transport phenomena in interacting particle systems.

Such an approach was recently taken by Ueba and coworkers[25−27] who have applied the NEGF formalism to the resonant level model of phonon assisted tunneling where a single bridge level represents a junction connecting two free electron reservoirs while being also coupled to a single harmonic mode. The free particle Hamiltonian is

$$\hat{H}_0 = E_1\hat{c}_1^\dagger\hat{c}_1 + \sum_{k\in L,R}\epsilon_k\hat{d}_k^\dagger\hat{d}_k + \Omega_0\hat{a}^\dagger\hat{a} \qquad (1)$$

where $\hat{c}_1^\dagger$ and $\hat{c}_1$ are creation and annihilation operators for electrons on the bridging level of energy E_1, $\{k\} = \{l\},\{r\}$ are sets of electronic states representing the left (L) and the right (R) electrodes with the corresponding creation and annihilation operators $\hat{d}_k^\dagger$ and $\hat{d}_k$, and $\hat{a}^\dagger$and $\hat{a}$ are creation

* Corresponding author. Tel: +972-3-6408904. Fax: +972-3-6423765. E-mail: Nitzan@post.tau.ac.il.

10.1021/nl049319y CCC: $27.50
Published on Web 07/30/2004

and annihilation operators for the phonon mode of frequency ω_0. The interactions are given by

$$\hat{H}_1 = \sum_{k\in L,R} (V_{k1}\hat{d}_k^\dagger \hat{c}_1 + hc) + M(\hat{a}^\dagger + \hat{a})\hat{c}_1^\dagger \hat{c}_1 \qquad (2)$$

Within this model Ueba et al. have reproduced and improved results obtained earlier by Persson and Baratoff.[17−19] In both treatments inelastic tunneling spectra are analyzed in the leading order M^2 of the electron phonon interaction. Persson and Baratoff have observed (following Davis[28]) that in this order there is an important correction to the elastic component of the tunneling current at the onset ($|e\Phi| = \hbar\Omega_0$ where Φ is the bias potential) of the inelastic channel. This contribution to the tunneling flux stems from what may be seen as interference between the purely elastic current amplitude that does not involve electron−phonon interaction and the elastic amplitude associated with two electron−phonon interaction events involving virtual phonon emission and absorption. Depending on the energetic parameters of the system, the resulting correction to the elastic current may be negative and, furthermore, may outweigh the positive contribution of the inelastic current, leading to a negative peak in the second derivative of the current/voltage relationship. Such negative features have indeed been observed in single-molecule vibrational spectroscopy of methyl isocyanide adsorbed on aluminia-supported rhodium particles[29] and of oxygen molecules chemisorbed on Ag(100).[7] The recent results by Reed and co-workers[13] that show relatively strong derivative-like features in the low-temperature IETS spectrum of C8 alkane thiols may be another manifestation of the same effect.

Spectroscopic line widths are often difficult to interpret since their origins may lie in diverse physical factors. In the recent IETS experiment by Wang et al.[13] it was found possible to eliminate or to estimate some of the important contributions of the thermal Fermi distribution in the substrate and of the distribution of the local electrostatic field and to come up with what the authors call an "intrinsic line width" of 3.73 ± 0.98 mV at $T = 4$ K in a nanojunction containing a layer of alkane C8 molecules between gold electrodes. As already mentioned, the rate of vibrational relaxation due to nuclear coupling with the thermal environment is expected not to exceed a few wavenumbers at near zero temperatures and cannot account for this observation. On the other hand, inhomogeneous broadening is obviously a possible contribution to the observed line width in a measurement such as of ref 13 that involves a sample of a few thousands molecules. For a molecule adsorbed on a metallic substrate, another channel of relaxation involves the vibronic coupling to the continuum of electron−hole pairs in the metal. Indeed, such coupling has been shown to be an important and sometimes dominating source of broadening in the infrared spectra of molecules adsorbed on metal surfaces.[18]

In this paper we apply the NEGF approach[30] to the analysis of line shapes and in particular line widths of IETS features. The model used in refs 25−27 is generalized to include coupling of the molecular bridge to its thermal environment. Furthermore, previous calculations are generalized by computing the inelastic tunneling flux to all orders in the vibronic coupling M, using the self-consistent Born approximation (SCBA).[31,32] We show that while the second-order approximation captures much of the essential physics of the IET process, infinite order corrections can lead to quantitative differences with qualitative implications, e.g., overtones in the IETS spectra that are absent in the low order theory are obtained in the infinite order treatment, and peaks (dips) in $d^2I/d\Phi^2$ vs. Φ spectrum, predicted by the low order theory, can appear as dips (peaks) in the infinite order calculation. At the same time, experimentally verifiable predictions can be made with respect to the dependence of the shapes and widths of the IETS vibrational features on the parameters that characterize the junction. In particular, using model parameters inferred from experimental information, we argue that the main intrinsic contribution to IETS line widths results from the coupling of molecular vibrations to electron−hole excitations in the lead(s) to which the molecule is chemically bonded.

Our model is defined by the Hamiltonian

$$\hat{H}_0 = E_1\hat{c}^\dagger\hat{c} + \sum_{k\in L,R} \epsilon_k \hat{d}_k^\dagger \hat{d}_k + \Omega_0 \hat{a}^\dagger\hat{a} + \sum_m \omega \hat{b}_m^\dagger \hat{b}_m \qquad (3)$$

where the four terms on the right-hand side represent, respectively, electrons on the molecules, electrons on the (left, L and right, R) leads, a primary molecular harmonic mode of frequency Ω_0, and a secondary subset of harmonic modes of frequencies ω_m that represent the thermal environment. The first three terms are the same as in eq 1. In the last term, $\hat{b}_m(\hat{b}_m^\dagger)$ represents the annihilation (creation) operators of the phonon bath modes. This zero order description is supplemented by the interaction Hamiltonian

$$\hat{H}_1 = \sum_{k\in L,R} (V_{k1}\hat{d}_k^\dagger \hat{c} + hc) + M\hat{A}\hat{c}^\dagger\hat{c} + \sum_m U_m \hat{A}\hat{B}_m \qquad (4)$$

where $\hat{A} = \hat{a}^\dagger + \hat{a}$ and $\hat{B}_m = \hat{b}_m^\dagger + \hat{b}_m$. The three terms in eq 4 correspond respectively to coupling between the bridge electronic system and the leads, on-bridge coupling of the primary phonon to the electronic system (the polaronic form used here corresponds to the assumption that the equilibrium position of the molecular vibration depends on whether the electron is on the molecule or on the metals), and interaction of the local phonon mode with its thermal environment. The phonon bath and the electronic reservoirs that represent the left and right electrodes are assumed to be at thermal equilibrium with temperature T;[33] however, the electronic electrochemical potentials μ_L and μ_R of the electrodes are different such that $\mu_L - \mu_R = e\Phi$ where e is the electron charge and Φ is the imposed bias potential. The wide band approximation is invoked for bridge−lead coupling and for the coupling between the bridge phonon and the thermal

environment, so that these couplings may be characterized by constant width parameters

$$\Gamma_K = 2\pi\sum_{k\in K}|V_{1k}|^2\delta(E_k - E_1);\ K = L,R \tag{5}$$

and

$$\gamma_{\rm ph} = 2\pi\sum_m |U_m|^2\delta(\omega_m - \Omega_0) \tag{6}$$

In addition, the coupling between the electronic and nuclear motions on the bridge is characterized by the parameter M in eq 4.

Orders of magnitudes of these parameters can be inferred from different experimental data. The width parameters $\Gamma_{\rm L}$ and $\Gamma_{\rm R}$ are related to observed lifetimes of excess electrons on molecules adsorbed on metal surfaces and can be estimated theoretically and from time-resolved 2-photon photoemission experiments (see, e.g., refs 34, 35) to be in the range 0.1−1 eV for chemisorbed species. $\gamma_{\rm ph}$ can be estimated from studies of vibrational relaxation (VR) of molecules embedded in cold matrices. VR rates depend strongly on the oscillator frequency, the bath spectrum, and the temperature; however, for our purpose it is sufficient to assert that for Ω_0 larger than the bath Debye frequency the corresponding width $\gamma_{\rm ph}$ at low T is generally less than 10^{-4} eV. Finally, the electron−phonon coupling M can be estimated in molecular systems from reorganization energies, $E_{\rm reorg} \approx M^2/\omega_0$, inferred from electron-transfer rate studies in similar environments. Observed values for $E_{\rm reorg}$ are 0.1−1 eV, and taking $\Omega_0 \sim 0.1$ eV places the magnitude of M in the range of a few tenths of eV.

Next we briefly outline our theoretical approach. We use the NEGF (Keldysh) formalism. The central objects that need to be evaluated are the electron and phonon Green's functions (GFs), G and D respectively, whose projections on the real time axis are

$$G^r(t,t') = -i\Theta(t-t')\langle\{\hat{c}(t),\hat{c}^+(t')\}\rangle;\ G^a(t,t') = i\Theta(t'-t)\langle\{\hat{c}(t),\hat{c}^+(t')\}\rangle \tag{7a}$$

$$G^<(t,t') = i\langle\hat{c}^+(t')\hat{c}(t)\rangle;\ G^>(t,t') = -i\langle\hat{c}(t)\hat{c}^+(t')\rangle \tag{7b}$$

$$D^r(t,t') = -i\Theta(t-t')\langle[\hat{A}(t),\hat{A}^+(t')]\rangle;\ D^a(t,t') = i\Theta(t'-t)\langle[\hat{A}(t),\hat{A}^+(t')]\rangle \tag{8a}$$

$$D^<(t,t') = -i\langle\hat{A}^+(t')\hat{A}(t)\rangle;\ D^>(t,t') = -i\langle\hat{A}(t)\hat{A}^+(t')\rangle \tag{8b}$$

At steady-state one can transform to the energy domain and solve self-consistently the Dyson equations for the retarded and advanced GFs

$$G^r(E) = ([G_0^r(E)]^{-1} - \Sigma^r(E))^{-1} \tag{9}$$

$$D^r(\omega) = ([D_0^r(\omega)]^{-1} - \Pi^r(\omega))^{-1} \tag{10}$$

(and same with $r \leftrightarrow a$) and the Keldysh equations for the lesser and greater projections

$$G^<(E) = G^r(E)\Sigma^<(E)G^a(E) \tag{11}$$

$$D^<(\omega) = D^r(\omega)\Pi^<(\omega)D^a(\omega) \tag{12}$$

(and same with $<\leftrightarrow>$). Σ is the electron self-energy that, for the present model Hamiltonian, expresses the consequence of the interaction of the electron on the bridge with the external electronic reservoirs on the electrodes and with its phonon environment. Π is the self-energy of the primary phonon, expressing the consequence of its interaction with the phononic thermal environment as well as with the electronic subsystem. In the so-called "non-crossing" approximation,[36] the corresponding contributions are assumed additive, i.e., using obvious notation

$$\Sigma(E) = \Sigma_{\rm L}(E) + \Sigma_{\rm R}(E) + \Sigma_{\rm ph}(E) \tag{13}$$

$$\Pi(\omega) = \Pi_{\rm ph}(\omega) + \Pi_{\rm el}(\omega) \tag{14}$$

$\Sigma_{\rm L}$ and $\Sigma_{\rm R}$, the components of the electronic self-energy Σ associated with the coupling to the left and right leads, are given in the wide band approximation by[37]

$$\Sigma_K^r = \Sigma_K^{a*} = -(1/2)i\Gamma_K \tag{15a}$$

$$\Sigma_K^< = i\Gamma_K f_K(E) \tag{15b}$$

$$\Sigma_K^> = -i\Gamma_K[1 - f_K(E)] \tag{15c}$$

where $K = L,R$ denote the left and right leads, $f_K(E)$ are the Fermi−Dirac distributions for the left and right electrodes, characterized by the corresponding chemical potentials μ_K, $f_K(E) = [\exp[(E-\mu_K)/k_{\rm B}T] + 1]^{-1}$, and Γ_K is defined by eq 5. In the same wide band approximation, the phonon-bath contribution to the self-energies of the primary phonon takes the forms

$$\Pi_{\rm ph}^r(\omega) = -(1/2)i{\rm sgn}(\omega)\gamma_{\rm ph} \tag{16a}$$

$$\Pi_{\rm ph}^<(\omega) = -i\gamma_{\rm ph}F(\omega) \tag{16b}$$

$$\Pi_{\rm ph}^>(\omega) = -i\gamma_{\rm ph}F(-\omega) \tag{16c}$$

where

$$F(\omega) = \begin{cases} N(|\omega|) & \omega > 0 \\ 1 + N(|\omega|) & \omega < 0 \end{cases};\ N(\omega) = [\exp(\omega/k_{\rm B}T) - 1]^{-1} \tag{17}$$

The phonon contribution to the electronic self-energy and the electronic contribution to the self-energy of the primary

phonon may be represented, within the self-consistent Born approximation (SCBA),[31,38] in terms of the electron and phonon GFs. The corresponding expressions are

$$\Sigma^r_{ph}(E) = i|M|^2 \int \frac{d\omega}{2\pi}[D^<(\omega)G^r(E-\omega) + D^r(\omega)G^<(E-\omega) + D^r(\omega)G^r(E-\omega)] - i|M|^2 D^r(\omega=0)\int \frac{dE}{2\pi}G^<(E) \quad (18a)$$

$$\Sigma^<_{ph}(E) = i|M|^2 \int \frac{d\omega}{2\pi}D^<(\omega)G^<(E-\omega) \quad (18b)$$

$$\Sigma^>_{ph}(E) = i|M|^2 \int \frac{d\omega}{2\pi}D^>(\omega)G^>(E-\omega) \quad (18c)$$

$$\Pi^r_{el}(\omega) = -i|M|^2 \int \frac{dE}{2\pi}[G^<(E)G^a(E-\omega) + G^r(E)G^<(E-\omega)] \quad (19a)$$

$$\Pi^<_{el}(\omega) = -i|M|^2 \int \frac{dE}{2\pi}G^<(E)G^>(E-\omega) \quad (19b)$$

$$\Pi^>_{el}(\omega) = -i|M|^2 \int \frac{dE}{2\pi}G^>(E)G^<(E-\omega) \quad (19c)$$

Equations 9−14, 18, 19 may be solved self-consistently. The procedure starts with the expressions for the Green's functions of the electronic system and the primary phonons that are zero order in the electron−phonon interaction and, at each iteration step until convergence, updates the electron and phonon self-energies using the GFs obtained in the previous iteration step. The numerical calculation of these Green functions and self-energies involves repeated integrations over the electronic energy E and the frequency variable ω. These are done using numerical grids that are chosen large enough to span the essential energy and frequency regions of the corresponding spectra, and dense enough relative to the spectral widths to yield reliable quadratures.[39] For more discussion of the theory and for details of the numerical procedure, see ref 30.

After convergence is achieved, the resulting Green functions and self-energies can be used to calculate many important characteristics of the junction. In particular, the total current through the junction is given by

$$I_{L(R)} = \frac{2e}{\hbar}\int \frac{dE}{2\pi}\mathrm{Tr}[\Sigma^<_{L(R)}(E)G^>(E) - \Sigma^>_{L(R)}(E)G^<(E)] \quad (20)$$

Here $I_{L(R)}$ is the current at the left (right) molecule-lead contact. It can be shown that $I_L = -I_R$ in accordance with Kirchoff's law. Using eq 11 and the assumed additive form (eq 13) of the electronic self-energy, the total current eq 20 can be recast as a sum of elastic and inelastic contributions written below at the left contact:

$$I_{el} = \frac{2e}{\hbar}\int \frac{dE}{2\pi}\mathrm{Tr}[\Sigma^<_L(E)G^r(E)[\Sigma^>_L(E)+\Sigma^>_R(E)]G^a(E) - \Sigma^>_L(E)G^r(E)[\Sigma^<_L(E)+\Sigma^<_R(E)]G^a(E)] = \frac{2e}{\hbar}\int_{-\infty}^{\infty}\frac{dE}{2\pi}(f_L(E)-f_R(E))Tr[\Gamma_L(E)G^r(E)\Gamma_R(E)G^a(E)] \quad (21)$$

$$I_{inel} = \frac{2e}{\hbar}\int \frac{dE}{2\pi}\mathrm{Tr}[\Sigma^<_L(E)G^r(E)\Sigma^>_{ph}(E)G^a(E) - \Sigma^>_L(E)G^r(E)\Sigma^<_{ph}(E)G^a(E)] \quad (22)$$

A common approximation to these results is obtained by considering only terms up to second order in the electron−phonon interaction M. In this case the GFs in eq 22 are replaced by their zero-order counterparts, while Σ_{ph} is taken from the lowest order equivalent of eq 18 in which the GFs G and D are represented by their zero order counterparts:

$$I^{(2)}_{inel} = \frac{2e}{\hbar}\int \frac{dE}{2\pi}\mathrm{Tr}[\Sigma^<_L(E)G^r_0(E)\Sigma^>_{ph,0}(E)G^a_0(E) - \Sigma^>_L(E)G^r_0(E)\Sigma^<_{ph,0}(E)G^a_0(E)] \quad (23)$$

To obtain eq 21 in the same order, the GFs are expressed by the lowest order Dyson forms

$$G^r(E) = G^r_0(E) + G^r_0(E)\Sigma^r_{ph,0}(E)G^r_0(E) \text{ (and same for } r \leftrightarrow a) \quad (24)$$

to get

$$I^{(0)}_{el} + I^{(2)}_{el} = \frac{2e}{\hbar}\int_{-\infty}^{\infty}\frac{dE}{2\pi}(f_L(E)-f_R(E))Tr[\Gamma_L(E)G^r_0(E)\Gamma_R(E) G^a_0(E)] + \frac{2e}{\hbar}\int_{-\infty}^{+\infty}\frac{dE}{2\pi}(f_L(E)-f_R(E))Tr[\Gamma_L(E)G^r_0(E)\Sigma^r_{ph,0}(E) G^r_0(E)\Gamma_R(E)G^a_0(E) + hc] \quad (25)$$

Equations 23 and 25 were recently used by Mii et al.[26] to rederive the results of Persson and Baratoff[18,19] for the IETS spectra for a model of a single electronic level connecting between the leads (in this case all GFs and self-energies are scalars and the trace operation in eqs 23 and 25 is unneeded). In the examples displayed below, we compare the results of this lowest order perturbation theory (LOPT) approximation to the full SCBA calculation.

Next we use the theoretical tools presented above to estimate the effect of vibronic coupling on the line width of vibrational features in IETS. Since a truly intrinsic line width can be observed only in a single molecule measurement, the relevant energy parameters are those suitable to an STM experiment, i.e., $\Gamma_L \ll \Gamma_R$ and E_1 essentially pinned to the Fermi energy of the right electrode. However, in what follows we consider the general case represented by keeping E_1 pinned to the unbiased Fermi energy and moving the

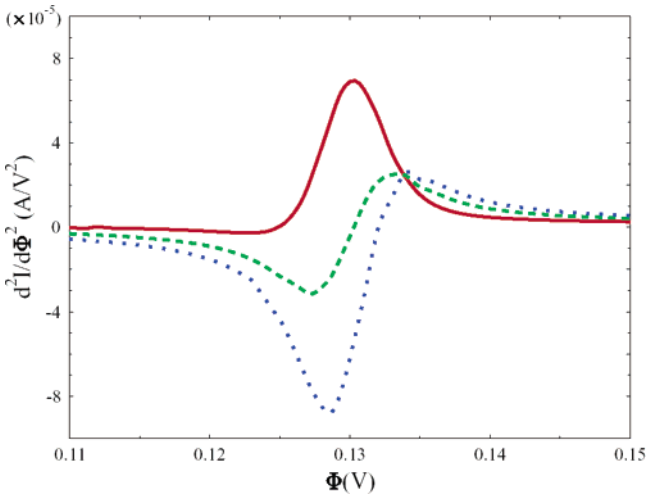

Figure 1. The IETS threshold feature in $d^2I/d\Phi^2$ for the model defined by eqs 3 and 4 using $\Gamma_L = \Gamma_R = 0.5$ eV, $\gamma_{ph} = 0.0001$ eV, $M = 0.3$ eV and $T = 10$ K. Full line (red) $E_1 = 0.70$ eV, dashed line (green) − $E_1 = 0.60$ eV, dotted line (blue) − $E_1 = 0.55$ eV.

chemical potentials of the left and right electrodes with a "voltage division factor"[40,41] η according to

$$\mu_L = E_F + \eta|e|\Phi$$
$$\mu_R = E_F - (1-\eta)|e|\Phi \qquad (26)$$

The STM limit, with the left electrode representing the tip, is given by $\eta \rightarrow 1$. In the calculations displayed below we have taken E_F as the energy origin, i.e., $E_F = 0$, and have used the model $\eta = \Gamma_R/\Gamma$ that implies stronger pinning of the molecular level to the electrode that provides larger electronic coupling.

IETS spectra are usually displayed as the second derivative of the current with respect to the bias voltage plotted against this voltage. Within the present formalism the low-temperature structure of this spectrum may be investigated by starting from $I = I_{el} + I_{inel}$ and using the $T = 0$ limits of eqs 21 and 22. It can be shown[26,30] that, provided that $\Gamma_{tot} \gg \gamma_{tot}$ where $\Gamma_{tot} \equiv \Gamma_L + \Gamma_R - 2\mathrm{Im}\Sigma^r_{ph}(E)$ and $\gamma_{tot}(\omega) \equiv \gamma_{ph} + \gamma_{el}(\omega)$ with $\gamma_{el}(\omega) = -2\mathrm{Im}\Pi^r_{el}(\omega)$, $d^2I/d\Phi^2$ is characterized by fundamental and overtones of a threshold ($|e|\Phi = \hbar\Omega_0$) feature whose width is of the order $\gamma_{tot}(|e|\Phi)$ and whose shape (peak, dip, peak-derivative-like) depends on the junction parameters. A demonstration of the latter statement is shown in Figure 1 (see also Figure 1 of ref 25) in which this fundamental feature is displayed for different choices of the resonance energy E_1. We note that, in principle, E_1 can be controlled by a gate electrode.

In what follows, consider the low-temperature width of this vibrational feature. Focusing on the electronic contribution $\gamma_{el}(\omega = |e|\Phi)$, we use the formalism described above to compute the electronic self-energy of the bridge phonon that yields this contribution via its imaginary part. Unless otherwise stated, we use as a representative set of bridge parameters the values $\Gamma_L = 0.05$ eV, $\Gamma_R = 0.5$ eV, $\gamma_{ph} = 0.0001$ eV, $M = 0.3$ eV, $E_1 = 1$ eV, and $\Omega_0 = 0.13$ eV. The voltage distribution is taken according to eq 26 with $\eta = \Gamma_R/\Gamma$. The temperature is taken $T = 10$ K; however, we find that the result for γ_{el} is practically independent of T up to room temperature.[42]

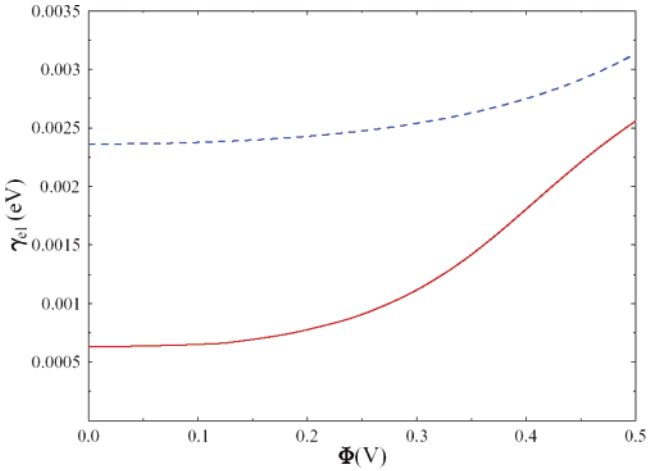

Figure 2. The electronic contribution $\gamma_{el}(\Phi)$ to the imaginary part of the vibrational self-energy plotted against the bias potential Φ. Full line: SCBA results. Dashed line: Lowest (second) order perturbation theory. See text for parameters.

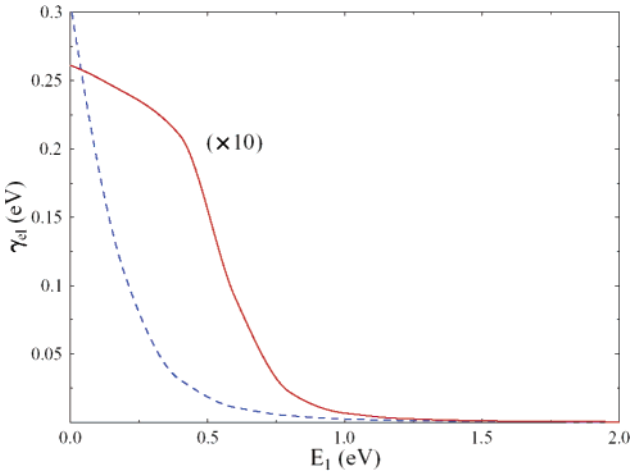

Figure 3. The electronic contribution $\gamma_{el}(\Phi = \omega_0/e)$ to the width of the IETS signal plotted against the position E_1 of the bridge level relative to the Fermi energy E_F of the unbiased junction. Full line: SCBA results (multiplied by a factor 10). Dashed line: Lowest (second) order perturbation theory. See text for parameters.

Figures 2−5 show the results obtained for the dependence of γ_{el} on the parameters that characterize the junction. (The total IETS width is given by $\gamma_{tot} = \gamma_{ph} + \gamma_{el}$ to which γ_{ph} makes a small fixed contribution.) Figure 2 shows the voltage dependence. Physically meaningful values of γ_{el} correspond to the threshold voltage, $|e|\Phi = \hbar\Omega_0$, at which the vibrational feature is observed. At this range and for our choice of molecular parameters γ_{el} is not strongly sensitive to the applied voltage. This suggests that the shape of the corresponding IETS feature is not strongly affected by this dependence. The other figures display the dependence of the electronic contribution to the total line width, γ_{el} evaluated at $|e|\Phi = \hbar\Omega_0$, on the parameters that characterize the molecular junction: the position of the resonance energy E_1 (Figure 3), the coupling to the tip (left) electrode (Figure 4),

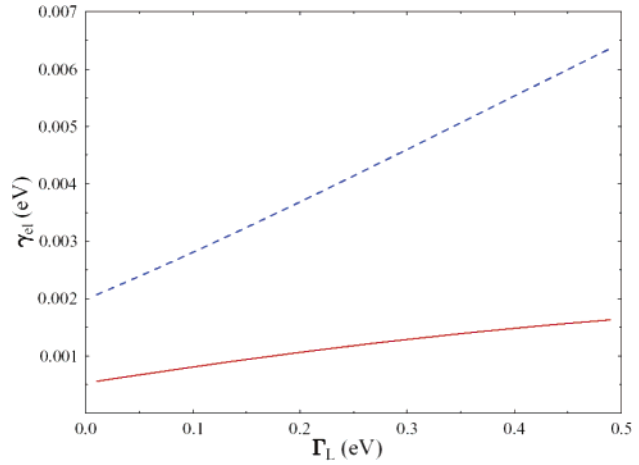

Figure 4. Same as Figure 3, where γ_{el} evaluated at $\Phi = \omega_0/e$ is plotted against the width Γ_L of the bridge level that results its coupling to the tip (left electrode).

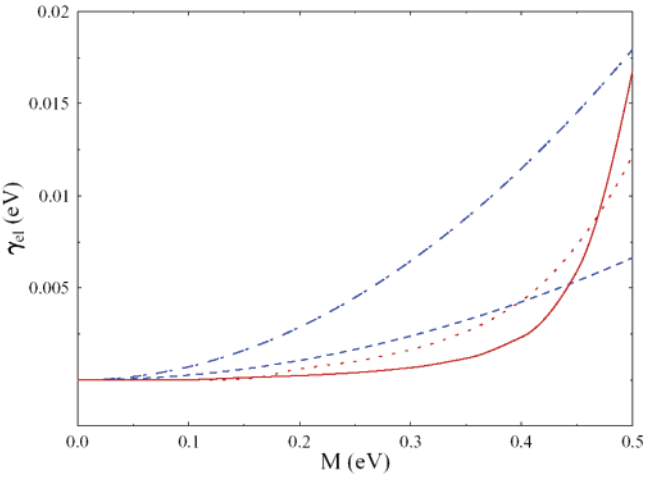

Figure 5. $\gamma_{el}((\Phi = \omega_0/e)$ plotted against the electron−phonon coupling strength M using parameters given in the text. Full and dotted lines are SCBA results obtained for $\Gamma_L = 0.05$ eV and 0.5 eV, respectively. Dashed and dash−dotted lines are 2nd order perturbation theory results for $\Gamma_L = 0.05$ eV and 0.5 eV, respectively.

and the strength of the electron−phonon coupling (or the corresponding reorganization energy $E_{reorg} = M^2/\Omega_0$, Figure 5).

The following points are noteworthy. (1) γ_{el} decreases with increasing spacing E_1 between the Fermi energy of the unbiased junction and the electronic resonance energy of the bridge. As already noted, E_1 may be varied, at least in principle, by a gate electrode. This dependence, most pronounced at higher E_1 may provide a way to identify cases where the observed width is indeed dominated by this contribution. (2) γ_{el} depends mildly on Γ_L, a parameter that may be varied by changing the tip−molecule distance. For $\Gamma_L = \Gamma_R = 0.5$ eV, values typical to experimental situations such as that of ref 13, the electronic contribution to the IETS width exceeds 1 meV, close to the order of magnitude deduced from this experiment. (3) The variation of γ_{el} with the electron−phonon coupling M changes from a relatively mild dependence at small M to a rapid increase when M increases beyond ~0.4 eV, the order of magnitude of Γ. We should, however, keep in mind that for large electron−phonon coupling the validity of even the SCBA level of computation is uncertain. (4) For our choice of electron−phonon coupling, $M = 0.3$ eV, substantial differences are observed between the SCBA results and those obtained in second-order perturbation theory, which is used in standard treatments of IETS. The observations made above are based on the SCBA results. (5) As was already mentioned γ_{el} is only very weakly sensitive to the temperature. Obviously, however, at higher temperatures, other contribution to the overall width will dominate the IETS line width.

In conclusion, based on the simple model described above and using a reasonable choice of parameters, we have found that the coupling of molecular vibrational modes to the electronic continua of the leads (via the molecular vibronic coupling) makes a substantial contribution of the order of ~1 meV to the width of IETS spectra. This is expected to be the largest source of broadening in low temperatures single molecule IETS spectra; however, in experiments such as that of ref 13 that involve a few thousand molecules, one cannot rule out inhomogeneous contributions as the dominating source of broadening. We have also shown that IETS line shapes and line widths depend on junction parameters, in particular the position of the bridge electronic resonance that can be affected by a gate voltage and the molecule lead coupling that can be controlled by the tip-molecule distance in a scanning tunneling spectroscopy setup.

Another observation, of technical nature, concerns the use of second-order perturbation theory in these applications. Comparing calculations done on this level of approximation to results obtained from the SCBA theory, we may conclude that second order perturbation theory can account only qualitatively for the effects discussed above. With typical molecular coupling parameters, the SCBA calculation seems to yield reliable results as long as the electron−primary phonon interaction is not too large.

Acknowledgment. M.R. thanks the DoD/MURI initiative, the NASA URETI program and the NSF NCN program for support. A.N. thanks the Israel Science Foundation, the U.S.−Israel Binational Science Foundation and the Volkswagen Foundation for support. A.N. thanks Prof. Jan van Ruitenbeek (Leiden University) for illuminating discussions.

References

(1) Wolf, E. L. *Principles of electron tunneling spectroscopy*; Oxford University Press: New York, 1985; Vol. 71.
(2) Hipps, K. W.; Mazur, U. *J. Phys. Chem.* **1993**, *97*, 7803.
(3) Lee, H. J.; Ho, W. *Science* **1999**, *286*, 1719.
(4) Lorente, N.; Persson, M.; Lauhon, L. J.; Ho, W. *Phys. Rev. Lett.* **2001**, *86*, 2593
(5) Hahn, J. R.; Ho, W. *Phys. Rev. Lett.* **2001**, *87*, 196102.
(6) Lauhon, L. J.; Ho, W. *Phys. Rev. Lett.* **2000**, *85*, 4566.
(7) Hahn, J. R.; Lee, H. J.; Ho, W. *Phys. Rev. Lett.* **2000**, *85*, 1914.
(8) Gaudioso, J.; Laudon, J. L.; Ho, W. *Phys. Rev. Lett.* **2000**, *85*, 1918.
(9) Stipe, B. C.; Rezaei, M. A.; Ho, W. *Phys. Rev. Lett.* **1999**, *82*, 1724.
(10) Lauhon, L. J.; Ho, W. *Phys. Rev. B* **1999**, *60*, R8525.
(11) Zhitenev, N. B.; Meng, H.; Bao, Z. *Phys. Rev. Lett.* **2002**, *88*, 226801.
(12) Park, H.; Park, J.; Lim, A. K. L.; Anderson, E. H.; Alivisatos, A. P.; McEuen, P. L. *Nature* **2000**, *407*, 57.
(13) Wang, W.; Lee, T.; Kretzschmar, I.; Reed, M. A. *Nano Lett.* **2004**, *4*, 643.

(14) Kushmerick, J. G.; Lazorcik, J.; Patterson, C. H.; Shashidhar, R.; Seferos, D. S.; Bazan, G. C. *Nano Lett.* **2004**, *4*, 639.
(15) Lee, H. J.; Ho, W. *Phys. Rev. B* **2000**, *61*, R16347.
(16) Smit, R. H. M.; Noat, Y.; Untiedt, C.; Lang, N. D.; Hemert, M. C. V.; Ruitenbeek, J. M. V. *Nature* **2002**, *419*, 906.
(17) Persson, B. N. J. *Phys. Scripta* **1988**, *38*, 282.
(18) Baratoff, A.; Persson, B. N. J. *J. Vac. Sci. Technol. A* **1988**, *6*, 331.
(19) Persson, B. N. J.; Baratoff, A. *Phys. Rev. Lett.* **1987**, *59*, 339.
(20) Troisi, A.; Ratner, M. A.; Nitzan, A. *J. Chem. Phys.* **2003**, *118*, 6072.
(21) Keldysh, L. V. *Sov. Phys. JETP* **1965**, *20*, 1018.
(22) Kadanoff, L. P.; Baym, G. *Quantum Statistical Mechanics. Green's Function Methods in Equilibrium and Nonequilibrium Problems*; Benjamin: Reading, MA, 1962.
(23) Wagner, M. *Phys. Rev. B* **1991**, *44*, 6104.
(24) Datta, S. *Electric transport in Mesoscopic Systems*; Cambridge University Press: Cambridge, 1995.
(25) Mii, T.; Tikhodeev, S. G.; Ueba, H. *Phys. Rev. B* **2003**, *68*, 205406.
(26) Mii, T.; Tikhodeev, S.; Ueba, H. *Surf. Sci.* **2002**, *502*−*503*, 26.
(27) Tikhodeev, S.; Natario, M.; Makoshi, K.; Mii, T.; Ueba, H. *Surf. Sci.* **2001**, *493*, 63.
(28) Davis, L. C. *Phys. Rev. B* **1970**, *2*, 1714.
(29) Bayman, A.; Hansma, P.; Kaska, W. C. *Phys. Rev. B* **1981**, *24*, 2449.
(30) Galperin, M.; Ratner, M. A.; Nitzan, A., to be published.
(31) Mahan, G. D. *Many-particle physics*, 3rd ed.; Plenum Press: New York, 2000.
(32) Haug, H.; Jauho, A.-P. *Quantum Kinetics in Transport and Optics of Semiconductors*; Springer: Berlin, 1996; Vol. 123.
(33) Our analysis, as well the earlier work of Person and Baratoff[17−19] and its reassessment by Ueba and co-workers,[25−27] correspond to the limit where electron transmission across the junction is a low probability event that does not disturb the thermal equilibrium in the leads. In the opposite limit where the lead−bridge coupling is strong so that the transmission probability is nearly 1 (implying a single channel conduction of $e^2/\pi\hbar$), we may encounter the situation where in the negatively biased bridge backscattered electrons of energies in the conduction window between the left and right Fermi energies are locally depleted near the junction. This causes increased reflection at the onset of inelastic scattering, which is presumably the dominant mechanism for observed negative peaks in point contact spectroscopy characterized by large transmission probabilities, see e.g., R. H. M. Smit, et al. *Nature* **2002**, *419*, 906; N. Agraït, et al. *Phys. Rev. Lett.* **2002**, *88*, 216803.
(34) Gauyacq, J. P.; Borisov, A. G.; Raseev, G. *Surf. Sci.* **2001**, *490*, 99.
(35) Kinoshita, I.; Misu, A.; Munakata, T. *J. Chem Phys.* **1995**, *102*, 2970.
(36) Wingreen, N. S.; Meir, Y. *Phys. Rev. B* **1994**, *49*, 11040.
(37) This should provide a reasonable simplification provided that the molecular electronic level is far enough (relative to its width Γ) from the metal band edge. The same assumption used for the phonon bath in eq 16 is generally valid because of the smallness of the vibrational width γ.
(38) Migdal, A. B. *Sov. Phys. JETP* **1958**, *7*, 996.
(39) Other workers have used SCBA for similar applications, see, e.g., Hyldgaard, P.; Hershfield, S.; Davies, J. H.; Wilkins, J. W. *Ann. Phys.* **1994**, *236*, 1. Our calculation goes beyond that done by these authors in several ways: first, we do not limit it to zero temperature, second, we calculate the nonequilibrium behavior of both electron and primary phonon systems while these authors assume that the phonon remains in equilibrium; and finally, most important in the present context, we address the electronic contribution to the phonon self-energy as part of the self-consistent calculation—a step that was not done before.
(40) Datta, S.; Tian, W. D.; Hong, S. H.; Reifenberger, R.; Henderson, J. I.; Kubiak, C. P. *Phys. Rev. Lett.* **1997**, *79*, 2530.
(41) Tian, W. D.; Datta, S.; Hong, S. H.; Reifenberger, R.; Henderson, J. I.; Kubiak, C. P. *J. Chem. Phys.* **1998**, *109*, 2874.
(42) Indirect dependence on temperature could come from the fact that γ_{ph} is often strongly temperature dependent, however we find that γ_{el} is also quite insensitive the magnitude of γ_{ph} up to values of tens of wavenumbers for the latter.

NL049319Y